



Zinc/Aluminum layered double hydroxide–titanium dioxide composite nanosheet film as novel solid phase microextraction fiber for the gas chromatographic determination of valproic acid

Amir Abbas Matin^{a,*}, Pourya Biparva^{b,*}, Hatam Amanzadeh^c, Khalil Farhadi^c

^a Department of Chemistry, Faculty of Sciences, Azarbijan Shahid Madani University, P.O. Box 53714-161, Tabriz, Iran

^b Department of Basic Sciences, Sari Agricultural Sciences and Natural Resources University, Sari, Iran

^c Department of Chemistry, Faculty of Science, Urmia University, Urmia, Iran

ARTICLE INFO

Article history:

Received 14 June 2012

Received in revised form

7 October 2012

Accepted 8 October 2012

Available online 16 October 2012

Keywords:

Valproic acid

Layered double hydroxide

Nanosheet

Solid phase microextraction

Gas chromatography

ABSTRACT

A nanosheet thin film based on Zn/Al layered double hydroxide (LDH) and TiO₂ composite was prepared via sol–gel process on capillary glass rod. Characterization of the fiber coating using X-ray diffraction (XRD) pattern and scanning electron microscopy (SEM) images showed that it consists of a large number of intercrossed and curved nanosheets with hexagonal architecture. The thickness of these plates is about few nanometers, and the lateral dimension is varying from 400 to 1000 nm. Application of the proposed coating as a solid phase microextraction fiber was investigated. As a model analyte, valproic acid (VPA, antiepileptic drug) was selected and its extraction from biological (human serum) and pharmaceutical (tablet and syrup) samples were performed without any considerable matrix effect. Analytical merits of the method, under optimum conditions (extraction temperature: 50 ± 1 °C, extraction time: 15 min, desorption temperature: 250 °C, desorption time: 2 min, solution pH: 1.5, salt concentration: 5 mol L^{−1}), are 70 µg L^{−1} and 0.20–100 mg L^{−1} for LOD and LDR, respectively.

© 2012 Elsevier B.V. All rights reserved.

1. Introduction

In recent years, considerable attention has been focused on synthesis of new materials, namely nanocomposites, to be employed as delivery vehicle for the removal of contaminated waste, electrochemical display devices, molecular electronics, heterogeneous catalysis and the controlled release of substances such as drugs, cosmetics and dyes. The field of nanocomposites involves the study of multiphase solid materials where at least one of the constituent phases has one dimension less than 100 nm, or structures having nano-scale repeated distances between the different phases that make up the material [1,2]. Nanomaterials have large specific surface areas, and thus a large fraction of active sites are available for appropriate chemical interaction. Recently many research groups have used nanomaterials for analyte extraction in biological and chemical analysis [3–6]. Compared with traditional sorbents, nanomaterials possess large surface area and short diffusion route, which may result in high extraction efficiency and rapid extraction dynamics.

For several decades, there has been a major expansion in the development of new nanoporous materials. One of them, which have attracted interest, is the pillared clays and their calcined products [7]. Layered double hydroxides (LDHs), also known as “anionic clay” and hydrotalcite-like compounds, belong to a special class of synthetic two-dimensional inorganic materials with lamellar structures and are one of the popular inorganic hosts for the formation of an organic–inorganic hybrid type nanolayered composite, or the so-called nanocomposite materials [8]. These compounds may be classified as neutral layers which are held together by van der Waals interactions, negatively charged layers which are separated by mobile cations, and positively charged layers which are separated by anions [9,10]. The chemical composition of LDHs are expressed by the general formula $[M_1^{2+}_{1-x} M_2^{3+}_x (OH)_2]^{x+} [A_{x/n}^{n-} \cdot m H_2O]^{x-}$, where M_2^{2+} = divalent cation (Mg²⁺, Co²⁺, Ni²⁺, Cu²⁺, Zn²⁺, etc.) and M_3^{3+} = trivalent cation (Al³⁺, Cr³⁺, Ga³⁺ etc.) while A^{n-} is the charge balancing interlayer anion. Heavy metals, such as Ni²⁺, Co²⁺, Cr³⁺, Ga³⁺, may be used to make LDH nanocomposites, but these metals have potential toxicity to the environment while the combination of Zn²⁺ and Al³⁺ is generally considered environmentally friendly. The ability of LDHs (as well as their calcination products) to adsorb inorganic as well as organic anions makes these materials very attractive for applications in several technological areas such as catalysts, catalyst supports, flame retardants

* Corresponding authors.

E-mail addresses: matin@azaruniv.edu, matinchem@gmail.com (A.A. Matin), pb.biparva@gmail.com (P. Biparva).

[11–13] stabilizers [14], ion-exchange materials, sorbents, absorbers, pharmaceuticals [15–18] and drug storage/delivery agents [19].

Several synthetic methods have been used to synthesize hydrotalcites that include co-precipitation [20,21], hydrothermal [22], salt oxide method [23], urea reduction [24,25], electrochemical [26], and sol–gel technique [27]. The most frequently used methods are co-precipitation and urea reduction, while the sol–gel method is suitable for preparing inorganic thin films [28] with pores in the nanometer range.

Drug analyses are important for the quality control of pharmaceutical preparations and the continuing development of more effective drugs. Furthermore, confirmation and determination of drugs in biological fluids are important for pharmacokinetic studies and clarification of therapeutic and toxic effects. Valproic acid (VPA, 2-propylpentanoic acid) is a simple eight carbon branched-chain fatty acid with unique anticonvulsant properties which is relatively free of central nervous system side effects. It is useful in controlling a broad range of clinical seizure disorders, primarily the treatment of absence, tonic-clonic and myoclonic seizures [29]. It is used in the management of grand mal epilepsy and petit mal epilepsy in pediatric patients, often with other adjunctive therapeutic agents. VPA has also been administered under investigational conditions in the treatment of psychiatric and movement disorders, including Huntington's chorea [30]. Monitoring of VPA levels in patient serum or plasma is essential when there are changes in VPA dose, concomitant medication or clinical condition of patient [31]. Various methods have been reported in the literature for this purpose. Gas chromatography [32–34], liquid chromatography [34–37] and capillary electrophoresis [38–40] are the main reported techniques for the determination of VPA. Although HPLC methods are frequently applied for this analysis but due to volatile nature of VPA, GC is often preferred, offering unrivalled high resolution [41]. The bioanalytical component of a pharmacokinetic study requires sample treatments such as extraction, preconcentration and clean-up steps to improve sensitivity and selectivity.

Solid phase microextraction (SPME) is a solvent-free method of extracting analytes from a variety of matrices by partitioning of them between a liquid or gaseous sample and immobilized stationary phase. It uses a very simple setup and requires no additional instrumentation. It has been applied in many fields such as the analysis of volatile components in foods [42], plants [43], and in biological samples [44] to determine drugs and metabolites of clinical and pharmacological interest. The extraction efficiency of SPME is determined by the distribution of analytes between the matrix and the coating. Therefore, the most important part of the SPME device is the fiber coating itself. To date, a number of novel coatings have been developed for the extraction of different kinds of compounds, in addition to the commercially available SPME fibers [45–48]. However, these fibers still show some drawbacks such as lower thermal and chemical stability and higher cost; hence, their application is restricted to some extent [49].

In this work, for the first time a new type nano-structured SPME fiber, Zn/Al LDH–TiO₂ composite, was synthesized based on sol–gel technique. The morphology, stability and extraction properties of the novel coating film were assessed. The results indicate that Al₂O₃ and TiO₂ gel with aqueous solution of zinc to induce the formation of special hexagonal Zn/Al LDH nanosheets film on capillary glass substrate. A series of experiments were performed to evaluate the performance of the new sol–gel LDH coating material for the determination of valproic acid, one of the most used antiepileptic drugs, in human serum and dosage forms (tablets and syrup) by headspace solid phase microextraction which were then separated with an established GC system.

2. Experimental

2.1. Chemicals and reagents

Aluminum tri-*sec*-butoxide (Al-(O-*sec*-Bu)₃), zinc acetate dihydrate, methyl acetoacetate (MAcAc), isopropyl alcohol (*i*-PrOH), 1-octanoic acid (internal standard), titanium (IV) isopropoxide (Ti-(O-*i*-C₃H₉)₃), ethylacetate, sodium chloride, hydrochloric acid and sodium hydroxide were analytical grade and obtained from E. Merck (Darmstadt, Germany). Pure sodium valproate (Rouz Darou Co., Tehran, Iran) powder was a gift from Prof. A. Jouyban (School of Pharmacy, Tabriz University of Medical Science, Tabriz, Iran). Standard stock solution of sodium valproate (100 mg L⁻¹) was prepared by dissolving appropriate amounts of it in water. Calibration series were prepared by dilution of stock solution in water.

2.2. Apparatus

An Agilent 6890N GC (Agilent technologies, Wilmington, DE, USA) equipped with a flame ionization detector (FID) and a split/splitless injector with an Agilent tapered liner (4 mm i.d.) was used. Separations were performed on a J&W DB-WAX (polyethylene glycol) capillary column (30 m × 0.25 mm i.d., film thickness 0.25 μm). Temperature program for separation of VPA was started at 80 °C and held for 1 min, and then increased by 20 °C min⁻¹ to 240 °C and held for 5 min. Nitrogen was used as carrier and makeup gas with flow rates of 1.2 and 45 mL min⁻¹, respectively. The temperatures of the injection port and detector were set at 250 °C. Injections were performed in splitless mode. ChemStation software was used for data acquisition and processing. The surface morphology of the coating film was studied using digital microscopy imaging scanning equipment VEGA 3 SB (TESCAN Co., s.r.o., Brno, Czech Republic). The X-ray diffraction pattern of the Zn/Al LDH–TiO₂ composite was recorded by X-ray diffractometer (GBC Scientific equipment, Braeside VIC, Australia) using Ni-filtered Cu Kα radiation (λ_{Cu Kα} = 0.15418 nm) at 35.4 kV and 28 mA. A Labinc BV model L-81 hot plate-stirrer (Labinc, Breda, Netherlands) was used for temperature control and sample agitation. A Metrohm 744 pH meter (Metrohm, Herisau, Switzerland) was used for pH adjustment. A lab-made SPME device was used.

2.3. Preparation of Zn/Al LDH–TiO₂ composite nanosheet film coated SPME fiber

In this study, the Zn/Al LDH–TiO₂ composite nanosheet thin film grown on capillary glass rod (OD ~0.25 mm) prepared via sol–gel method according to the following procedure. First, capillary glass rod was pretreated with *i*-PrOH and ethylacetate to remove the pollutants on their surfaces, and then rinsed with HPLC grade methanol. Al-(O-*sec*-Bu)₃ was dissolved in *i*-PrOH and MAcAc was added to the resultant solution as a stabilizer. The solution was stirred at room temperature for 1 h to prepare Al₂O₃ sol solution. To prepare TiO₂ sol solution, Ti-(O-*i*-C₃H₉)₃ was dissolved in *i*-PrOH, and then MAcAc was added and stirred for about 1 h. Two obtained solutions were mixed and stirred for 10 min to prepare a homogeneous sol solution. Finally, a mixture of deionized water and *i*-PrOH was added drop wise to the solution for hydrolysis and mixture was continuously stirred for 1 h. The molar ratio of the components in the final solution was Ti-(O-*i*-C₃H₉)₃:Al-(O-*sec*-Bu)₃:*i*-PrOH:Water = 1:1:20:4. After preparation of coating solution, capillary glass substrate was immersed in it and TiO₂/Al₂O₃ film was formed on the surface of the glass substrate by the dip-coating method at room temperature. Then, coated glass substrate was immersed in hot aqueous solution (~95 °C) of zinc acetate (0.015 mol L⁻¹) for 10 min. After drying in air flow, glass substrate was dried in an oven at 70 °C for 24 h and then thermally treated by

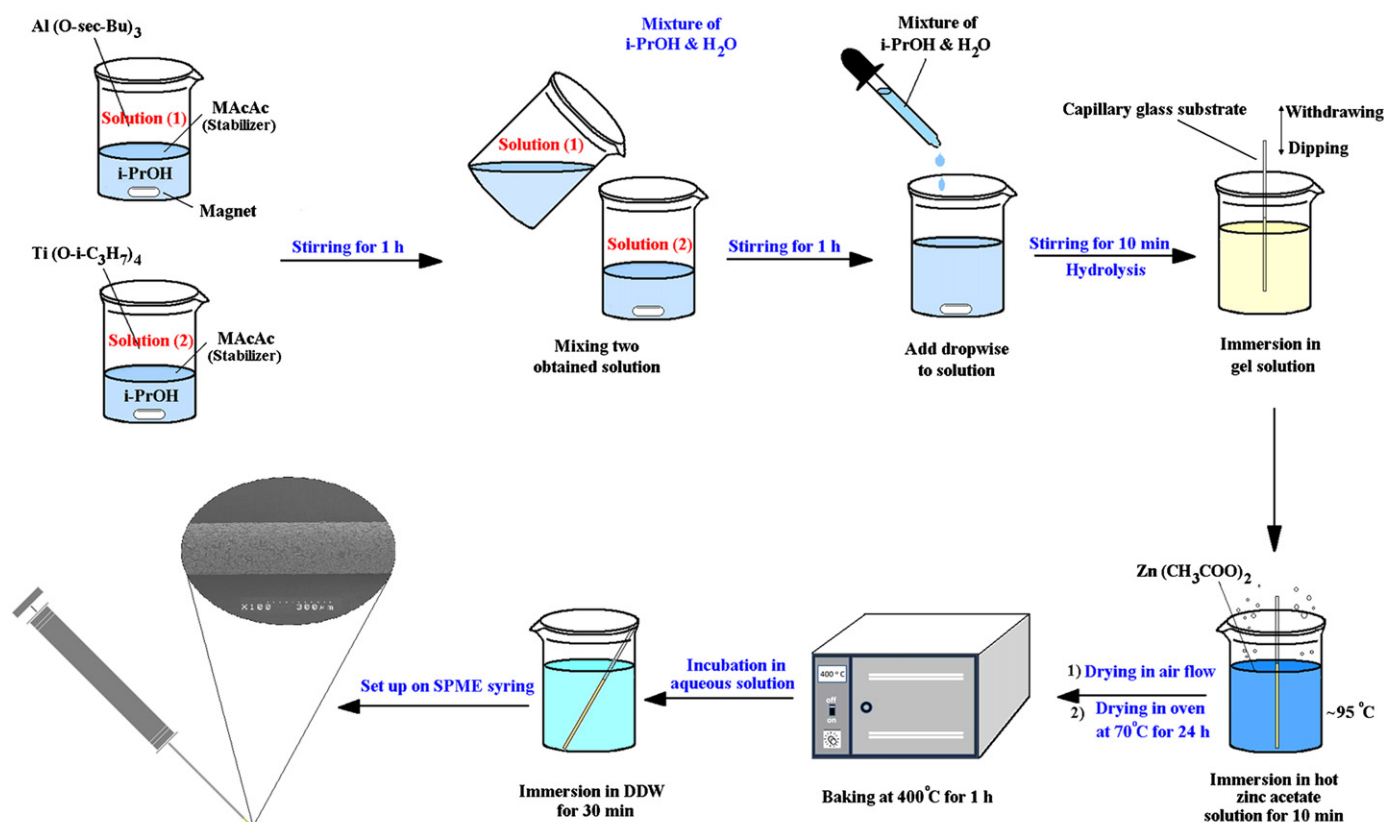


Fig. 1. Schematic illustration of fiber preparation process.

baking at 400 °C for an hour, and subsequent immersion in deionized distilled water (DDW) for 30 min. As final step, coated glass rod was installed on SPME device. Schematic procedure of fiber preparation was illustrated in Fig. 1.

2.4. Solid phase microextraction procedure

500 μL serum of a healthy person (without epilepsy) obtained from a medical diagnostic laboratory was transferred into the 10 mL volumetric flask, was spiked with a known amounts of VPA and 1-octanoic acid (internal standard) and was diluted to the mark with 5 mol L^{-1} sodium chloride solution. After pH adjustment at 1.5, obtained solution was transferred to a 15 mL vial containing a magnetic stir bar (PTFE coated). The vial was sealed with a PTFE-faced septum and an aluminum cap. Afterward, the vial was heated in a water bath (temperature was adjusted at 50 ± 1 °C) and agitated by a magnetic stirrer. Extraction was performed by exposing proposed fiber to the headspace of the sample for 10 min. After extraction, desorption of the analyte was performed in the hot injection port (250 °C) of GC for 2 min. For real samples of patients with epilepsy, the same procedure was done without drug spiking. In the case of drug formulations, 5 mg L^{-1} solution of tablet and syrup samples were prepared by dissolution of appropriate amounts of them in water and the microextraction were performed according to the procedure.

3. Results and discussion

3.1. Characterization of Zn/Al LDH–TiO₂ composite nanosheet film

Characterization of synthesized Zn/Al LDH–TiO₂ composite was performed in order to get better sight into the structural

properties of the adsorption matrix using X-ray diffraction (XRD) and scanning electron microscopy (SEM). The XRD diagram was recorded in the 5–80° (2θ) range at a scan speed of $2\theta = 10^\circ \text{ min}^{-1}$ and a time constant of 1 s. The XRD pattern of the Zn/Al LDH–TiO₂ nanocomposite (Fig. 2) shows sharp and symmetric peaks at lower 2θ values, which are characteristics of hydrotalcite-like compounds, and the material consists of a well-crystallized layered phase [50]. Fig. 3 illustrates the SEM images of the nanosheet film on glass substrates at different magnifications. High-magnification SEM image in Fig. 3c illustrates that coating composite consists of a large number of intercrossed and curved nanosheets which are similar to those building blocks of hexagonal (Fig. 3(c) insert) LDH plates architecture in LDH film. The thickness of these plates is about few nanometers and the lateral dimension is varying from 400 to 1000 nm.

3.2. Selection of SPME fiber substrate

In recent investigations, use of metallic bases like stainless steel wire as support for SPME fiber are preferred due to its high mechanical durability. Therefore, Zn/Al LDH–TiO₂ nanosheet film was prepared on both the glass rod and stainless steel wire for comparison. Results show that prepared film on metallic wire is not stable and can be easily washed away during the extraction or injection process, and the glass surface is suitable for the direct growth of Zn/Al LDH–TiO₂ composite nanosheet film. Therefore, capillary glass rod was selected for preparation of SPME fiber.

3.3. Selection of microextraction temperature and time

Temperature is one of the important factors affecting extraction equilibrium especially in headspace mode. Elevated temperatures influence the distribution constant of the analytes

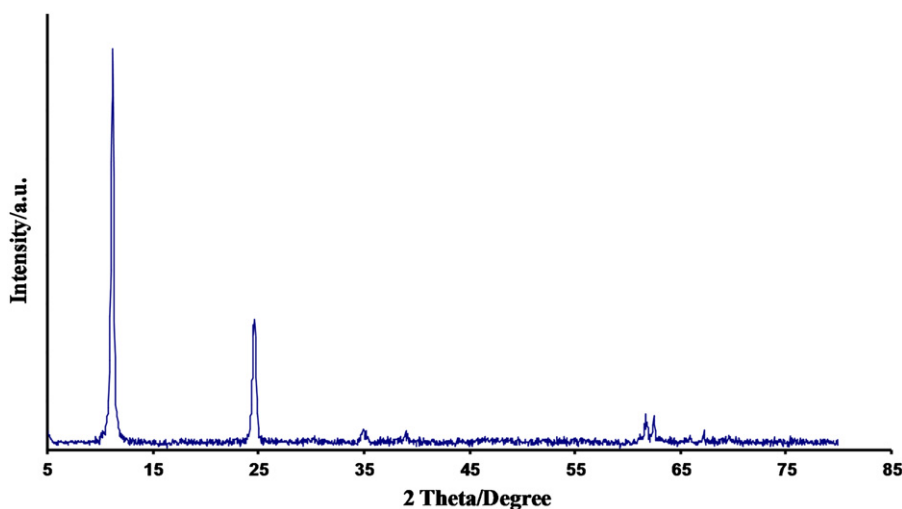


Fig. 2. XRD pattern of Zn/Al LDH-TiO₂ composite.

between sample solution and headspace which causes an increase in mass-transfer rate of the analytes from the sample matrix to the headspace phase. On the other hand, at high temperatures distribution constant of the analytes between headspace and the fiber is affected negatively. Thus, due to this contrast selection of the best extraction temperature as a critical parameter is very important. Evaluation of temperature effect was performed by varying the temperature from 20 to 70 °C.

As shown in Fig. 4, the amount of extracted drug increases with increasing solution temperature up to 50 °C. At temperatures higher than 50 °C extraction yield decreases significantly. So, 50 °C was selected as the best microextraction temperature. In the case of microextraction time, it is well known that the exposure time of the fiber in the headspace of samples is another effective parameter that was investigated in the range of 1 to 20 min. It is usually maintained long enough to achieve equilibrium between the headspace and the adsorbent. Results showed that amount of the extracted analyte reached to the maximum within 15 min, and it was selected as the best extraction time.

3.4. Selection of desorption temperature and time

It is well known that mechanism of analyte introduction to GC using SPME is thermal desorption from fiber surface in hot injection port of the GC. So for quantitative transfer of the analytes, desorption temperature must be optimized. For this purpose, injections were performed at various temperatures varying from 150 to 300 °C. According to the results, 250 °C is the best desorption temperature. Time of fiber duration in injection port of the GC is also important. Fast desorption provides sharper peaks and increases the separation efficiency. Experimental studies of desorption times ranging from 0.5 to 10 min show that the time required to complete desorption is 2 min.

3.5. Salting out effect

Addition of an inorganic salt has often been used to enhance the activity coefficients of volatile components in aqueous solutions. This causes the increasing of analyte concentration in the headspace phase. The salts are also added to equalize the activity coefficients of analytes in different matrices [51]. The effect of this parameter was studied by performing microextraction process in both the absence and presence of sodium chloride (concentrations ranging from 0.5 to 6 mol L⁻¹). According to Fig. 5, the

results indicate that the maximum extraction efficiency can be obtained in the presence of 5 mol L⁻¹ sodium chloride and higher. Thus, it was selected for further experiments.

3.6. Effect of sample agitation rate on microextraction efficiency

Transfer of the analytes from solution bulk to the fiber surface needs some kinds of agitation. It can be performed by magnetic stirring, sonication and the like. In this case, we used magnetic stirring at different agitation rates (0–700 rpm) and the best results obtained at 700 rpm.

3.7. Effect of solution pH on the extraction efficiency

It is obvious that ionized species have a great tendency for remaining in aqueous phase and it is necessary to convert them to molecular form for extraction. This is simply possible by pH adjustment according to *pK_a*. VPA is a weak acid (*pK_a*=4.8) which can be found in aqueous solutions in molecular and dissociated forms. In this step, effect of the solution pH on the amount of extracted VPA was investigated in the range of 1.5–9 by adding hydrochloric acid or sodium hydroxide solutions. It can be predicted that pH values lower than *pK_a* are suitable for this purpose because VPA is a volatile organic acid and it can be easily transferred to the headspace phase in its molecular form. Results confirmed the predictions and as shown in Fig. 6 the amount of the extracted analyte reached the maximum at pH 1.5.

3.8. Method validation

In order to evaluate the precision of the method, five replicate determinations were performed using a single fiber, and the relative standard deviations were calculated. Also, for studying the fiber reproducibility, microextraction process was performed using four different fibers with equal dimensions. The relative standard deviations were 2.17, 5.18, and 9.73% for microextraction of VPA from tablet, syrup and serum samples using single fiber, respectively and 8.23% for fiber-to-fiber study, which indicates that repeatability of microextraction process and reproducibility of the fiber is acceptable (Table 1). The analytical merits of the proposed method were determined. Corresponding calibration curve ($A = 38.0C + 21.673$, A =peak area, C =concentration, mg L⁻¹) with a high correlation coefficient ($r = 0.9989$), low detection limit (70 µg L⁻¹) and a wide linear dynamic range (0.20–100 mg L⁻¹) made the proposed method suitable for quantification of the VPA

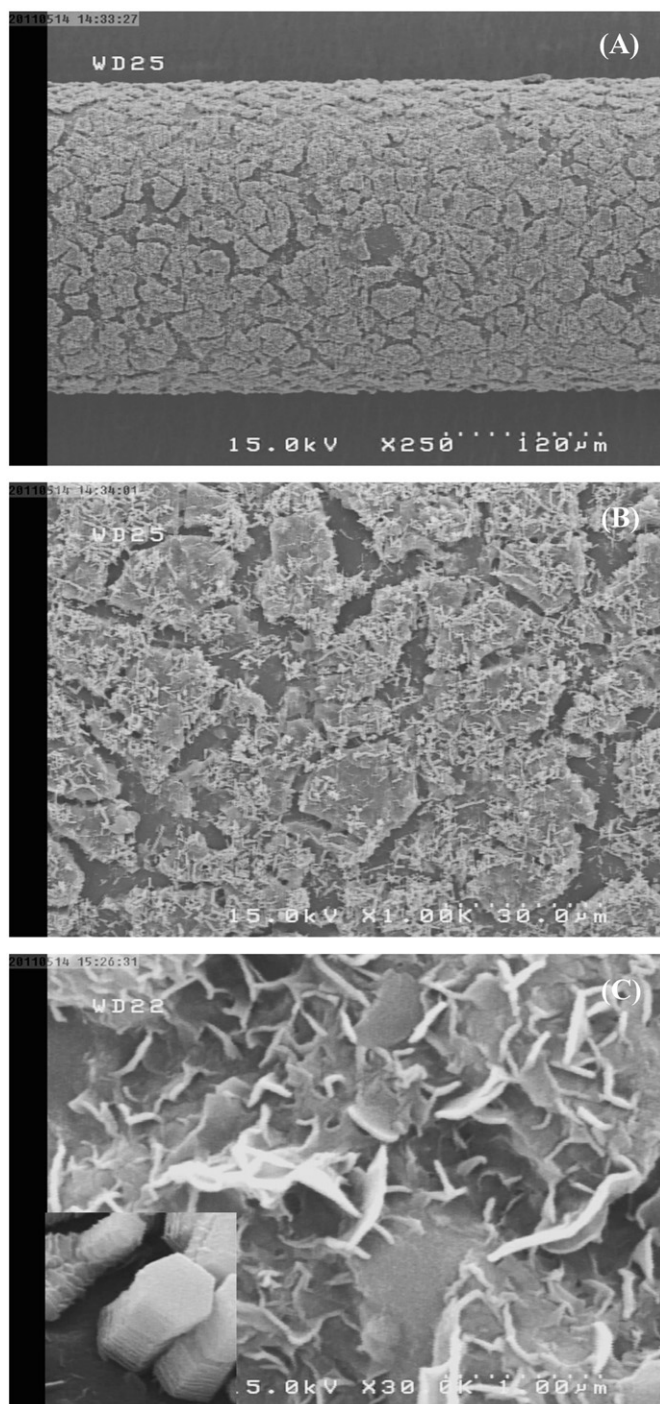


Fig. 3. SEM images of Zn/Al LDH-TiO₂ composite nanosheet at various magnifications (a) $\times 250$ (b) $\times 1,000$ (c) $\times 30,000$.

and comparable with those reported in the literature (Table 2). As can be seen, the LOD and LDR of the method using proposed fiber were improved.

3.9. Analysis of real samples

In order to evaluate method performance for the assay of VPA in real samples, a spiked human serum sample (10 mg L^{-1} of VPA) and serum sample of an epileptic patient were extracted and analyzed by GC-FID. Also, the method was applied for assay of VPA in tablets and syrup samples. The results are presented in Table 1. From recovery data in Table 1, it can be found that the

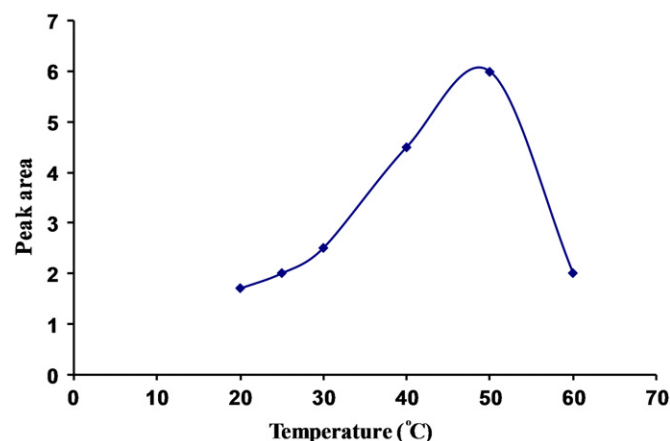


Fig. 4. Effect of temperature on microextraction efficiency. Extraction conditions: extraction time, 20 min; solution pH, 1.5; fiber length, 1.3 cm.

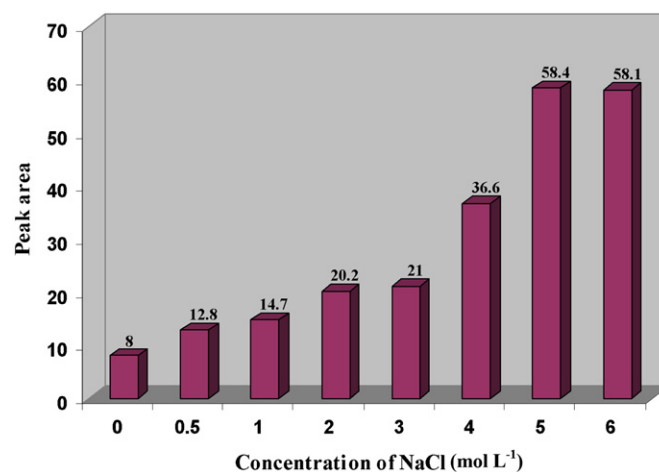


Fig. 5. Salting out effect on microextraction efficiency. Extraction conditions: extraction temperature, 50 °C; extraction time, 15 min; solution pH, 1.5; fiber length, 1.3 cm.

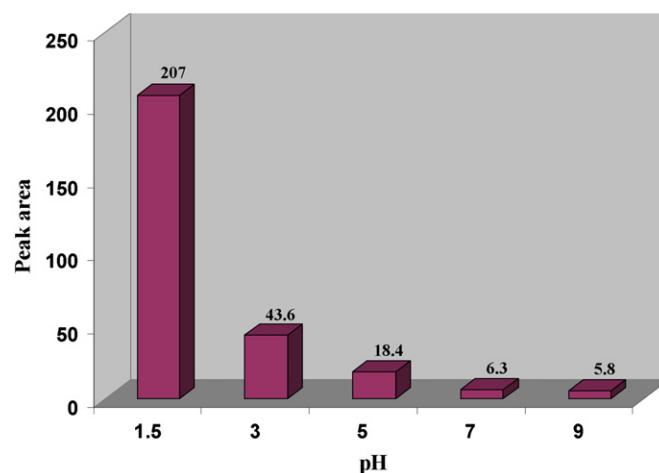


Fig. 6. Effect of pH on extraction efficiency. Extraction conditions: extraction temperature, 50 °C; extraction time, 15 min; fiber length, 1.3 cm; salt concentration, 5 mol L⁻¹.

proposed method is applicable for the determination of VPA in a complex matrix (serum) without a significant matrix effect. Fig. 7 shows typical chromatograms of drug samples. Figs. 7(a)–(c) present separation of VPA in standard solution (5 mg L^{-1}), tablet

Table 1
Results of real samples analysis and method repeatability.

Compound (matrix)	Labeled ^a /added ^b	Found \pm SD ^c	RSD (%) ^d	Recovery (%)
VPA (tablet)	200 mg	194.54 \pm 4.22 mg	2.17	97.27 \pm 2.11
VPA (syrup)	200 mg/5 mL	204.49 \pm 10.59 mg/5mL	5.18	102.24 \pm 5.29
VPA (serum) ^e	10 mg L ⁻¹	9.45 \pm 0.92 mg L ⁻¹	9.73	94.50 \pm 9.19
VPA (serum) ^f	–	2.50 \pm 0.18 mg L ⁻¹	7.20	–

^a Labeled content of pharmaceutical formulations.

^b Added quantity of drug into blank serum (mg L⁻¹).

^c Standard deviation.

^d Relative standard deviation for five replicate determinations with a single fiber.

^e Serum sampled from a healthy patient.

^f Serum sampled from an epileptic patient.

Table 2
Comparison of the proposed method with other methods reported in the literature.

Method	LOD ^a	LDR ^b	Ref.
HS-LPME ^c -GC-FID	0.80	2.0–20.0	[30]
HS-SPME-GC-FID	1.0	2.0–20.0	[29]
HS-SPME-GC-FID	0.085	0.25–100.0	[23]
HS-SPME-GC-FID	0.07	0.20–100.0	Proposed method

^a Limit of detection (mg L⁻¹).

^b Linear dynamic range (mg L⁻¹).

^c Liquid phase microextraction.

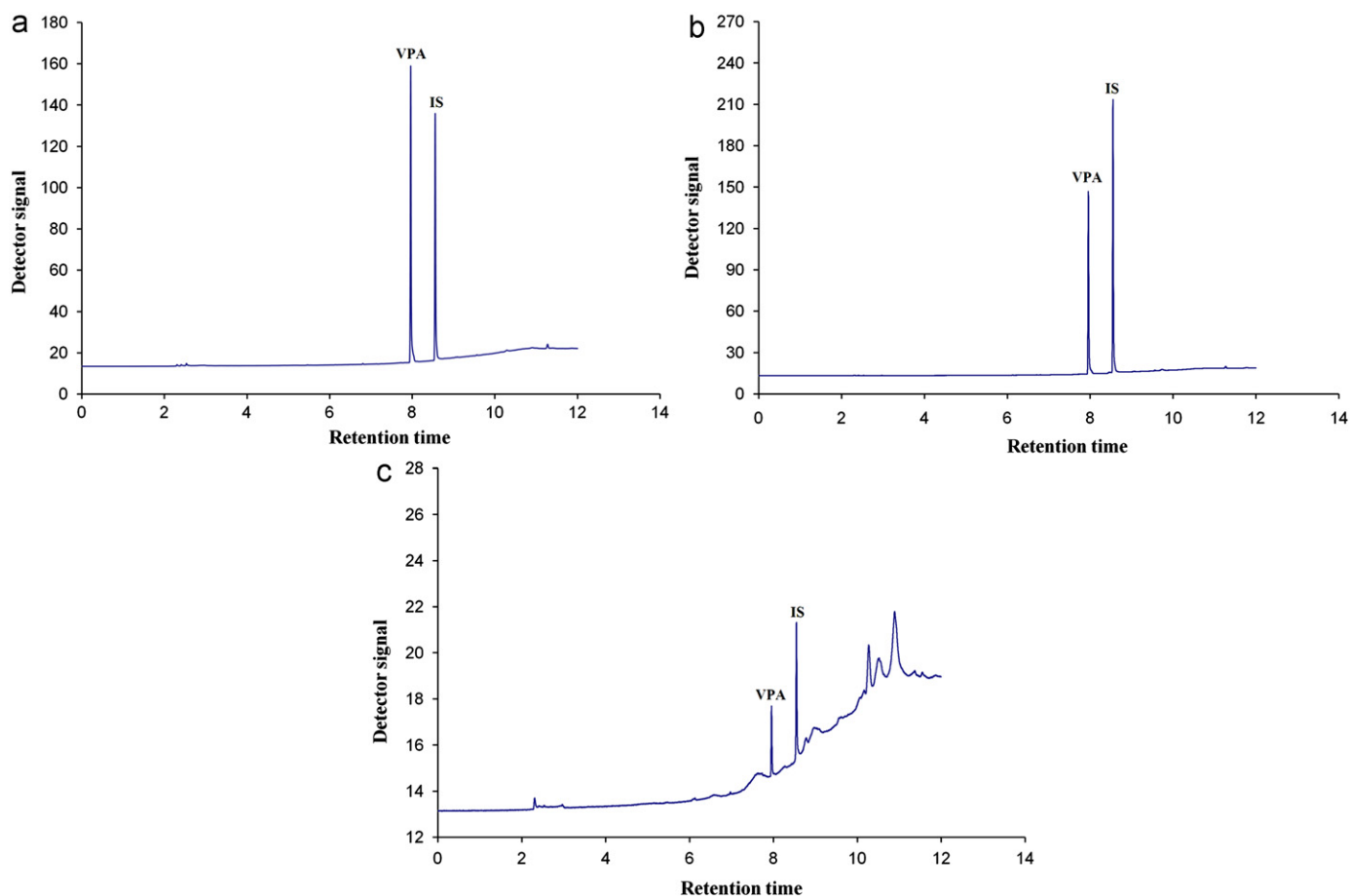


Fig. 7. Typical chromatograms of VPA in different samples (a) standard VPA solution, 5 mg L⁻¹ (b) tablet solution, 5 mg L⁻¹ and (c) spiked serum sample, 10 mg L⁻¹.

solution (5 mg L⁻¹) and spiked serum sample (10 mg L⁻¹), respectively. Also, existing of no interfering peaks in chromatograms of real samples show the ability of the method as an efficient clean-up technique.

4. Conclusion

In this study, a novel coating based on Zn/Al LDH-TiO₂ composite was prepared on glass substrate and its structure

was determined by XRD pattern and SEM images. Results confirm a layered nanosheet structure with hexagonal architecture. Application of proposed coating as an adsorbent material in solid phase microextraction of volatile polar organic compounds was investigated on valproic acid. After optimization of microextraction conditions, the proposed fiber was successfully used for therapeutic drug monitoring of VPA in human serum and quality control of drug in tablet and syrup formulations.

References

- [1] P.M. Ajayan, L.S. Schadler, P.V. Braun, Nanocomposite science and technology, Wiley VCH, Weinheim, Germany, 2003.
- [2] L. Perioli, T. Posati, M. Nocchetti, F. Bellezza, U. Costantino, A. Cipiciani, Appl. Clay Sci. 53 (2011) 374–378.
- [3] Y.Q. Cai, G.B. Jiang, J.Y. Liu, Q.X. Zhou, Anal. Chem. 75 (2003) 2517–2521.
- [4] H. Wang, A.D. Campiglia, Anal. Chem. 80 (2008) 8202–8209.
- [5] N. Savaga, M.S. Diallo, J. Nanopart. Res. 7 (2005) 331–342.
- [6] M.S. Diallo, S. Christie, P. Swaminathan, J.H. Johnson, Environ. Sci. Technol. 39 (2005) 1366–1377.
- [7] R.T. Yang, Adsorbents: Fundamentals and Applications, John Wiley & Sons Inc., New Jersey, 2003.
- [8] F. Kovanda, E. Jindová, K. Lang, P. Kubát, Z. Sedláková, Appl. Clay Sci. 48 (2010) 260–270.
- [9] U. Schubert, N. Husing, Synthesis of Inorganic Materials, Weinheim, Wiley-VCH, Germany, 2000.
- [10] A.R. Auxilio, P.C. Andrews, P.C. Junk, L. Spiccia, D. Neumann, W. Raverty, N. Vanderhoeck, Polyhedron 26 (2007) 3479–3490.
- [11] C. Nyambo, E. Kandare, D. Wang, C. Wilkie, Polym. Degrad. Stabil. 93 (2008) 1656–1663.
- [12] C. Nyambo, P. Songtipya, E. Manias, M. Jimenez-Gasco, C.A. Wilkie, J. Mater. Chem. 18 (2008) 4827–4838.
- [13] C. Manzi-Nshuti, D. Wang, J.M. Hossenlopp, C.A. Wilkie, J. Mater. Chem. 18 (2008) 3091–3102.
- [14] L. Van der Ven, M.L.M. van Gemert, L.F. Batenburg, J.J. Keern, L.H. Gielgens, T.P.M. Koster, H.R. Fischer, Appl. Clay Sci. 17 (2000) 25–34.
- [15] F. Cavani, F. Trifiro, A. Vaccari, Catal. Today 11 (1991) 173–301.
- [16] S. Cheng, Catal. Today 49 (1999) 303–312.
- [17] X. Duan, D.G. Evans, Applications of Layered Double Hydroxides, Springer Verlag, Berlin Heidelberg, 2006.
- [18] V. Rives, Layered Double Hydroxides: Present and Future, Nova Science Publishers, New York, 2001.
- [19] A.N. Ay, B. Karan, A. Temel, V. Rives, Inorg. Chem. 48 (2009) 8871–8877.
- [20] M.J. Climent, A. Corma, S. Iborra, K. Epping, A. Velty, J. Catal. 225 (2004) 316–326.
- [21] R.L. Frost, A.W. Musumeci, J. Colloid Interf. Sci. 302 (2006) 203–206.
- [22] S.L. Wang, L.Q. Qian, H. Xu, G.L. Lu, W.J. Dong, W.H. Tang, J. Alloy. Compd 76 (2009) 739–743.
- [23] E. Manova, D. Paneva, B. Kunev, C. Estournes, E. Riviere, K. Tenchev, A. Leustic, I. Mitov, J. Alloy. Compd 485 (2009) 356–361.
- [24] J.T. Klopogge, L. Hickey, R. Trujillano, M.J. Holgado, M.S. San Roman, V. Rives, W.N. Martens, R.L. Frost, Cryst. Growth Des. 6 (2006) 1533–1536.
- [25] K.L. Erickson, T.E. Bostrom, R.L. Frost, Mater. Lett. 59 (2005) 226–229.
- [26] L. Indira, M. Dixit, P.V. Kamath, J. Power Sources 52 (1994) 93–97.
- [27] T. Lopez, P. Bosch, E. Ramos, R. Gomez, O. Novaro, D. Acosta, F. Figueras, Langmuir 12 (1996) 189–192.
- [28] N. Yamaguchi, T. Nakamura, K. Tadanaga, A. Matsuda, T. Minami, M. Tatsumisago, Cryst. Growth Des. 6 (2006) 1726–1729.
- [29] W. Loscher, Prog. Neurobiol. 58 (1999) 31–59.
- [30] W.J. Taylor, M.H. Diers Caviness, MT(ASCP), M.A. Irving, A Textbook for the Clinical Application of Therapeutic Drug Monitoring, Abbott Laboratories, 1986.
- [31] S.A. Konig, J. Knolle, S. Friedewald, W. Koelfen, E. Longin, T. Lenz, D. Hannak, Epilepsia 44 (2003) 708–711.
- [32] M.A. Farajzadeh, A.A. Matin, K. Farhadi, P. Hashemi, A. Jouyban, Anal. Sci. 25 (2009) 875–879.
- [33] M. Nakajima, S. Yamato, K. Shimada, S. Sato, S. Kitagawa, A. Honda, J. Miyamoto, J. Shoda, M. Ohya, H. Miyazaki, Ther. Drug Monit. 22 (2000) 716–722.
- [34] P. Shahdousti, A. Mohammadi, N. Alizadeh, J. Chromatogr. B 850 (2007) 128–133.
- [35] M.C. Lin, H.S. Kou, C.C. Chen, S.M. Wu, H.L. Wu, J. Chromatogr. B 810 (2004) 169–172.
- [36] T. Mino, M. Nakajima, H. Wakabayashi, S. Yamato, K. Shimada, Anal. Sci. 17 (2001) 999–1001.
- [37] N.V.S. Ramakrishna, K.N. Vishwottam, S. Manoj, M. Koteswara, M. Santosh, J. Chidambara, B.R. Kumar, Rapid Commun. Mass. Spectrom. 19 (2005) 1970–1978.
- [38] G.K. Belin, S. Krahenbuhl, P.C. Hauser, J. Chromatogr. B 847 (2007) 205–209.
- [39] V. Ioffe, T. Kalendarev, I. Rubinstein, G. Zupkovitz, J. Pharmaceut. Biomed. Anal. 30 (2002) 391–403.
- [40] V. Pucci, R. Mandrioli, M.A. Raggi, Electrophoresis 24 (2003) 2076–2083.
- [41] D. Yu, J.D. Gordon, J. Zheng, S.K. Panesar, K.W. Riggs, D.W. Rurak, F.S. Abbott, J. Chromatogr. B 666 (1995) 269–281.
- [42] C.L. Artur, J. Pawliszyn, Anal. Chem. 62 (1990) 2145–2148.
- [43] F. Augusto, A.L.P. Valente, E.S. Tada, S.R. Rivellino, J. Chromatogr. A 873 (2000) 117–127.
- [44] E.H.M. Koster, C. Wemes, J.B. Morsink, G.J. de Jong, J. Chromatogr. B 739 (2000) 175–182.
- [45] D. Budziak, E. Martendal, E. Carasek, Anal. Chim. Acta 598 (2007) 254–260.
- [46] J.X. Wang, D.Q. Jiang, Z. Gu, X. Yan, J. Chromatogr. A 1137 (2006) 8–14.
- [47] V. Vickackaite, V. Ciukasovaite, Cent. Eur. J. Chem. 5 (2007) 727–738.
- [48] M. Kaykhaii, G.W. Dicoski, R. Smedley, J. Pawliszyn, P.R. Haddad, J. Chromatogr. A 1217 (2010) 3452–3456.
- [49] J.S. Camara, J.C. Marques, R.M. Perestrelo, F. Rodrigues, L. Oliveira, P. Andrade, M. Caldeira, J. Chromatogr. A 1150 (2007) 198–207.
- [50] L.V. Liang, Y. Wang, M. Wei, J. Cheng, J. Hazard. Mater. 152 (2008) 1130–1137.
- [51] D. Zuba, A. Parczewski, M. Rozanska, Proceeding of the 39th annual TIAFT meeting (2001) Prague, Czech Republic.